JOURNAL OF Materials CHEMISTRY

Photoelectrochromic heterosupramolecular assemblies

Joao Sotomayor,† Geoffrey Will and Donald Fitzmaurice*

Department of Chemistry, University College Dublin, Belfield, Dublin 4, Ireland

Received 7th October 1999, Accepted 16th November 1999

Heterosupramolecular assemblies based on modified transparent nanostructured TiO_2 (anatase) membranes are described. Exposure of these heterosupramolecular assemblies to visible light causes them to turn blue. Furthermore, if a negative potential is applied to the nanostructured TiO_2 membrane this blue color persists for hours. Because only those areas which have been irradiated are blue, and because the lifetime of the blue colored state depends on the potential applied to the nanostructured TiO_2 membrane, applications are foreseen for these photoelectrochromic materials.

Introduction

By analogy with a supermolecule,[1,2] a heterosupermolecule possesses the following attributes:[3–5] first, the intrinsic properties of the linked condensed phase and molecular components are not significantly perturbed; and second, the properties of the heterosupermolecule are not a simple superposition of the properties of the linked condensed phase and molecular components, *i.e.* there exists a well defined heterosupramolecular function. Also by analogy with an organized assembly of supermolecules,[6–8] an organized assembly of heterosupermolecules offers the prospect of heterosupramolecular function addressable on the nanometer scale.

With respect to devices based on supramolecular or heterosupramolecular function addressable on the nanometer scale, an equally important objective is modulation of the functional state of the constituent supermolecules or heterosupermolecules of an assembly. To fully meet this objective requires the ability to modulate a chemical or physical property of at least one of the constituent condensed phase or molecular components of the supermolecules or heterosupermolecules in the organized assembly. By comparison with a supramolecular assembly,[9–11] mainly because modulation of the properties of even nanometer-scale condensed phase components is an increasingly realizable goal,[12,13] effective function modulation of is a more immediate prospect for a heterosupramolecular assembly.

In one approach, the heterosupermolecules of an assembly are organized so that they build their own substrate (Scheme 1), termed an *intrinsic substrate*. Modulating a property of the intrinsic substrate, of necessity, modulates the same or a related property of the condensed phase component of each of the heterosupermolecules in the assembly. Since the function of a heterosupermolecule is determined by the properties of its constituent components, effective function modulation is expected and has been observed.[14–16] Furthermore, if the property of the intrinsic substrate can be monitored, then the modulation state of the heterosupermolecules in the assembly may be inferred.

An example of this approach is the assembly and organization of heterosupermolecules consisting of covalently linked TiO_2 nanocrystal, ruthenium complex and viologen components (Scheme 2).[16]

Effective function modulation, *via* the intrinsic substrate formed by the TiO_2 nanocrystal components, proved possible. Specifically, the direction of light-induced electron transfer within the heterosupramolecular assembly was modulated by potentiostatically determining the quasi-Fermi level of the intrinsic substrate and, therefore, also the quasi-Fermi level of the TiO_2 nanocrystal component of each heterosupermolecule. At positive applied potentials, visible light excitation of the ruthenium complex component results in electron transfer to the TiO_2 nanocrystal component (95%). At negative applied potentials, however, visible light excitation of the ruthenium complex component results in electron transfer to both the TiO_2 nanocrystal (48%) and viologen components (52%).

These and related studies,[16–20] have led to the development of heterosupramolecular assemblies based on transparent nanostructured TiO_2 (anatase) membranes modified by chemisorption of linked ruthenium complex and viologen components. Exposure of these heterosupramolecular assemblies to visible light causes them to turn blue. Furthermore, if a negative potential is applied to the nanostructured TiO_2 membrane this blue color persists for hours. Because it is only those areas that have been irradiated that become blue, and because the lifetime of the blue state depends on the potential applied to the nanostructured TiO_2 membrane, applications are foreseen for these photoelectrochromic materials.

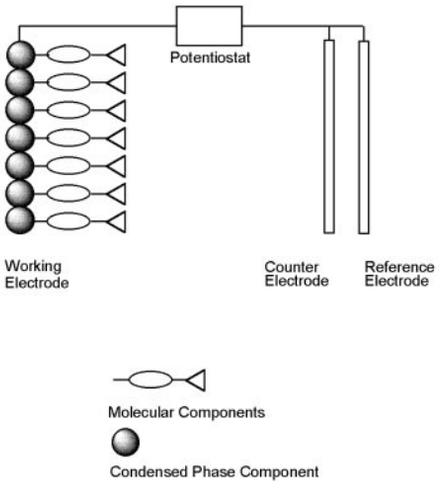

Scheme 1

†On sabbatical from the Centro de Quimica Fina e Biotecnologia, Departamento de Quimica, Faculdade de Ciencias e Tecnologia, Universidade Nova de Lisbona, Quinta de Torre, Monte de Caparica, 2825-114 Caparica, Portugal.

Experimental

Preparation of molecular components

The molecular components used in the present study $\mathbf{R^P}$, $\mathbf{R^PV^{C1}}$ and $\mathbf{R^PV^{C4}}$ are shown in Scheme 3. The preparation and characterization of these molecular components have been described elsewhere.[17]

All reagents were used as received from Aldrich. All solvents were Analar grade and also used as received. All ligands and molecular components were characterized by ^{1}H NMR spectra recorded on a JEOL JNM-GX270 FT spectrometer. Optical absorption spectra were measured using a Hewlett-Packard 8452A diode array spectrometer. Optical emission spectra were measured using a Perkin-Elmer 3000 fluorescence spectrometer. All elemental analysis was performed by the Chemical Services Unit at University College Dublin.

Preparation of transparent nanostructured TiO_2 membranes

Transparent nanostructured TiO_2 (anatase) membranes were prepared as described in detail elsewhere.[20] The thickness of a membrane was controlled by varying the concentration of the aqueous TiO_2 sol used. A sol containing 27 g dm^{-3} of TiO_2 gave rise, after having been fired in air at 450 °C for 24 h, to a transparent nanostructured TiO_2 membrane that was 58 μm thick and which, as may be seen from Fig. 1, was uniformly thick and free from cracking. Structural characterization of these membranes was by scanning electron microscopy (SEM), using a JEOL JSM 35C SEM, for samples mounted directly onto a conducting stub using quick drying silver paint (Agar Scientific Ltd.). Silver is known to form an ohmic contact to TiO_2.[21]

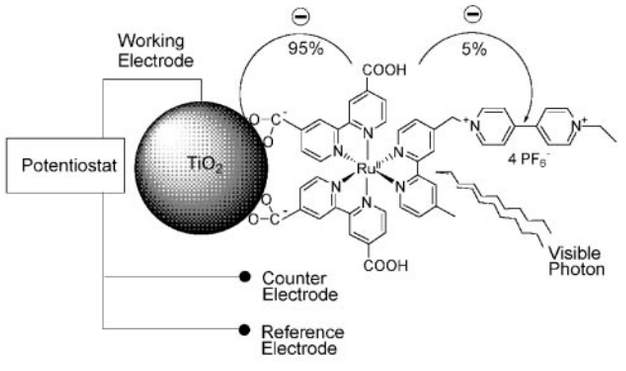

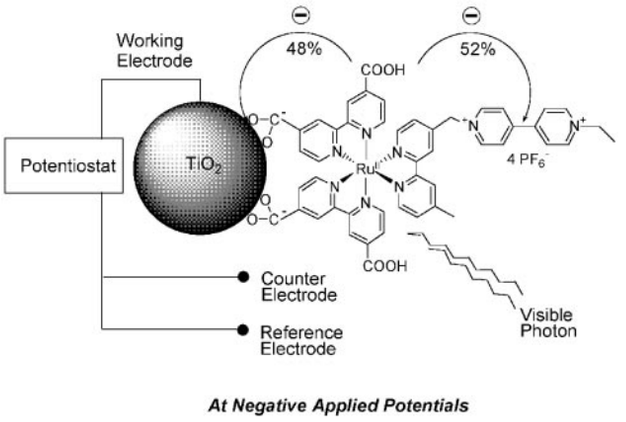

Scheme 2

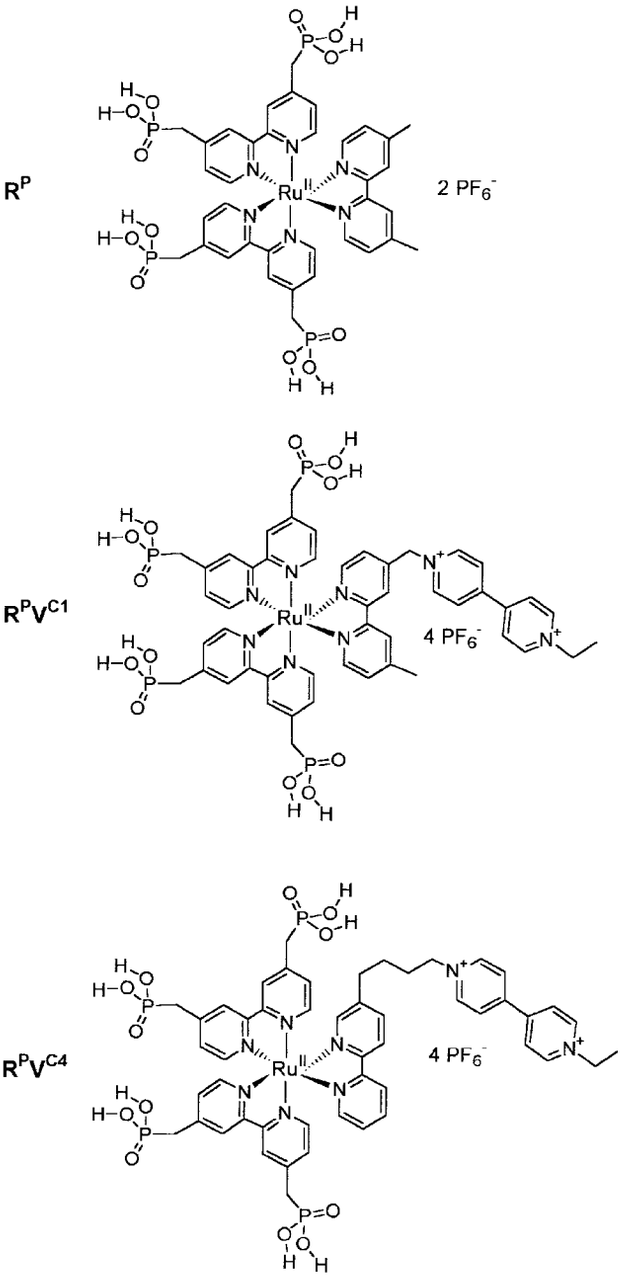

Scheme 3

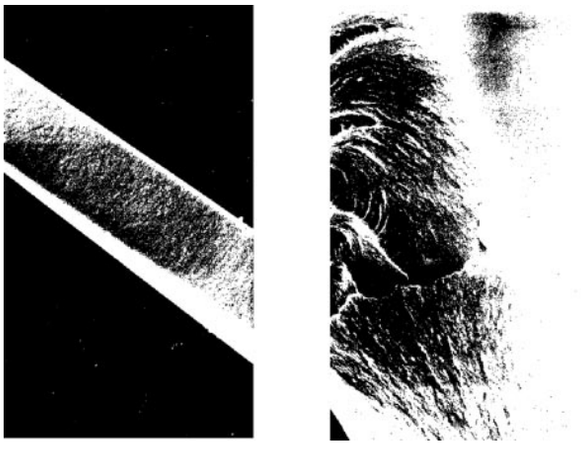

Fig. 1 Scanning electron micrograph of a 58 μm thick nanostructured TiO_2 membrane fired for 24 h.

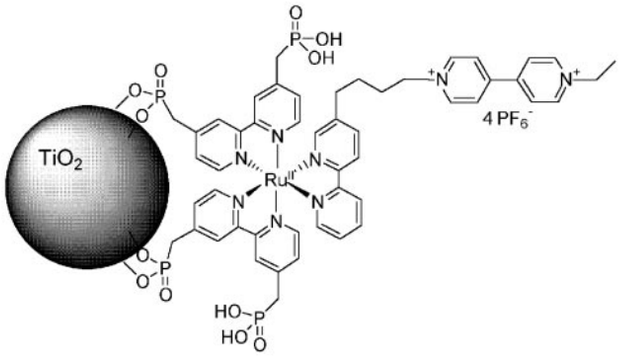

TiO_2-R^PV^{C4}

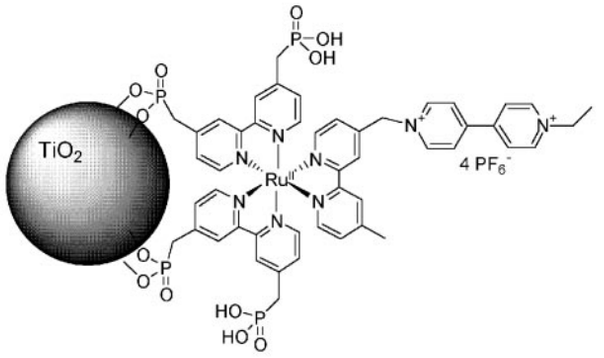

TiO_2-R^PV^{C1}

Scheme 4

Modification of transparent nanostructured TiO_2 membranes

A transparent nanostructured TiO_2 membrane was immersed in a saturated ethanolic solution containing $\mathbf{R^PV^{C1}}$ (2×10^{-5} mol dm^{-3}, pH 2.0) or $\mathbf{R^PV^{C4}}$ (2×10^{-5} mol dm^{-3}, pH 2.0) for 24 h. These membranes were subsequently washed thoroughly with ethanol and stored in a darkened vacuum desiccator prior to use. The resulting heterosupramolecular assemblies, denoted TiO_2–$\mathbf{R^PV^{C1}}$ and TiO_2–$\mathbf{R^PV^{C4}}$ respectively, are shown in Scheme 4. The use of phosphonic acid groups to link the ruthenium complex component to the surface of the constituent nanocrystals of the nanostructured TiO_2 membrane prevents their desorption at any applied potential for which results are reported.[17]

Potential dependent optical absorption spectroscopy of modified transparent nanostructured TiO_2 membranes

A modified nanostructured TiO_2 membrane was mounted on a platinum support using quick drying silver paint (Agar Scientific Ltd.). As has been noted, silver forms an ohmic contact to TiO_2.[21] A circular aperture (5 mm diameter) in the platinum support permitted the spectrometer beam to pass. This assembly formed the working electrode of a closed three-electrode single compartment cell constructed from a 1 cm × 1 cm quartz fluorimeter cuvette. The counter electrode was a flat platinum plate. The reference potential was provided by a $Ag/AgCl_{(sat)}$ mini-electrode. The electrolyte was $LiClO_4$ (0.2 mol dm^{-3}) in a MeCN–EtOH mixture (3 : 1, v/v). In all experiments, triethanolamine (TEOA) was added as a sacrificial donor (0.05 mol dm^{-3}). The electrolyte solution was degassed by bubbling with Ar for 20 min prior to measurement. Potential control was provided by a Solartron SI 1287 Electrochemical Interface. The cell described above was incorporated into the sample compartment of a Hewlett-Packard 8452A Diode Array Spectrophotometer.

Visible-light irradiation of modified transparent nanostructured TiO_2 membranes

The working electrode of the electrochemical cell, incorporated into the sample compartment of a Hewlett-Packard 8452A Diode Array Spectrophotometer, was irradiated for 3 s using the blue–green (488/514 nm) output of a Coherent Ar-ion laser (Innova 70-5) at 1000 mW cm^{-2} (corrected for reflection).

Results

Transparent nanostructured TiO_2 membranes

As stated, an aqueous sol of concentration 27 g dm^{-3} of TiO_2 gave rise to a transparent nanostructured TiO_2 membrane that was 58 μm thick. As may be seen from Fig. 1, this membrane was uniformly thick and free from cracking.

Following modification by chemisorption of $\mathbf{R^P}$ (2×10^{-5} mol dm^{-3} ethanolic solution, pH 2.0, 24 h), it was possible to estimate the surface roughness as 5000 for this membrane.[22]

Modification of transparent nanostructured TiO_2 membranes

Fig. 2 shows the optical absorption spectrum of a transparent nanostructured TiO_2 membrane prior to and following its modification by chemisorption of $\mathbf{R^PV^{C4}}$. Modification by chemisorption of $\mathbf{R^PV^{C1}}$ gives quantitatively similar results.

The following bands are observed between 350 and 800 nm:[23] a weak band at *ca.* 360 nm assigned to a metal centered (MC) d–d transition; a strong broad band at 460 nm assigned to a spin-allowed metal to ligand charge transfer (^{1}MLCT) d–π* transition and a long wavelength tail extending to about 600 nm assigned to a spin-forbidden (^{3}MLCT) d–π* transition. No bands that may be assigned to the **V** component are observed.

The band which dominates the visible absorption spectrum is the spin-allowed MLCT transition of the $\mathbf{R^P}$ component at 460 nm. The largely triplet excited state,[23] in which an electron is localized on one of the bipyridine ligands,[24] is formed by intersystem crossing in <300 fs.[25] It should be noted that the above electron, although initially localized on one of the three bipyridine ligands, hops between these ligands on the ps timescale.[26] If the $\mathbf{R^P}$ component is not linked to a TiO_2 nanocrystal or a **V** component, this ^{3}MLCT state undergoes radiative decay with a lifetime of the order of a few 100 ns, depending on the conditions, and gives rise to an emission spectrum with a maximum at 660 nm.[24] If, however, the $\mathbf{R^P}$ component is linked

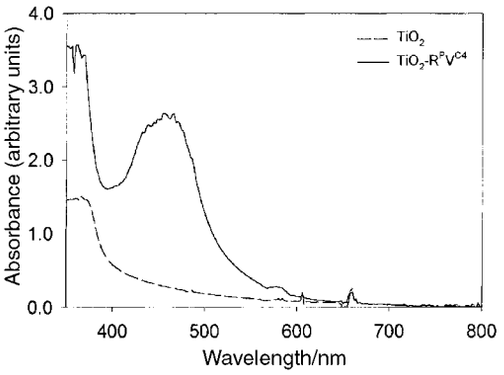

Fig. 2 Optical absorption spectra in air of a 58 μm thick nanostructured TiO_2 membrane fired for 24 h prior to and following adsorption of $\mathbf{R^PV^{C4}}$ from a saturated ethanolic solution (2×10^{-5} mol dm^{-3}, pH 2.0) during 24 h.

to a TiO_2 nanocrystal and a **V** component, as is the case in TiO_2–$\mathbf{R^PV^{C1}}$ and TiO_2–$\mathbf{R^PV^{C4}}$, the electron is transferred to the TiO_2 nanocrystal when localized on the bipyridine ligand linked to the nanocrystal,[27] and to the **V** component when localized on the bipyridine linked to the viologen. In neither case is emission observed.[24,28,29]

For a ruthenium complex chemisorbed at the surface of a nanostructured TiO_2 film and similar to that in TiO_2–$\mathbf{R^PV^{C1}}$ and TiO_2–$\mathbf{R^PV^{C4}}$, electron transfer to a nanocrystal by the complex in the ^{1}MLCT state is on the fs time-scale.[30] The reported values, generally upper limits, lie in the range of 25 to 150 fs.

For a supermolecule closely related to $\mathbf{R^PV^{C1}}$, a rate constant of 1.38×10^{11} s^{-1} for electron transfer from the electronically excited $\mathbf{R^P}$ component to the **V** component, corresponding to a lifetime of 7 ps, and a rate constant of 8.38×10^{10} s^{-1} for back electron transfer from the reduced **V** component to the oxidized $\mathbf{R^P}$ component, corresponding to a lifetime of 12 ps, have been measured by Mallouk and coworkers.[28]

For a supermolecule closely related to $\mathbf{R^PV^{C4}}$, a rate constant of 6.55×10^8 s^{-1} for electron transfer from the electronically excited $\mathbf{R^P}$ component to the **V** component, corresponding to a lifetime of 1500 ps, and a rate constant of 3.24×10^9 s^{-1} for back electron transfer from the reduced **V** component to the oxidized $\mathbf{R^P}$ component, corresponding to a lifetime of 300 ps, have also been measured by Mallouk and coworkers.[28] A similar rate constant of 6.2×10^8 s^{-1} for electron transfer from the electronically excited $\mathbf{R^P}$ component to the **V** component has been measured by Balzani and coworkers.[31]

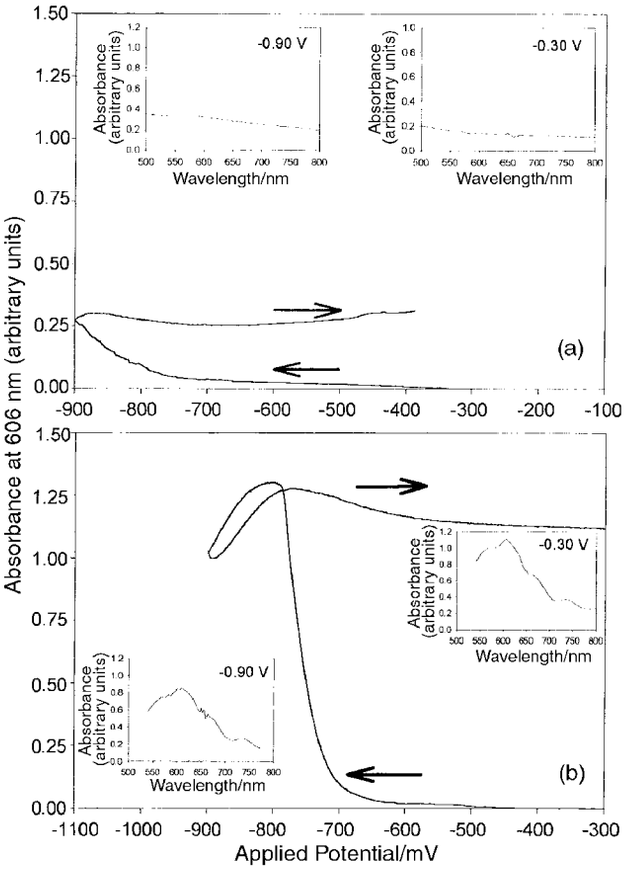

Fig. 3 Potential dependent optical absorption at 606 nm of a 58 μm thick nanostructured TiO_2 membrane fired for 24 h (a) prior to and (b) following adsorption of $\mathbf{R^PV^{C4}}$ from a saturated ethanolic solution (2×10^{-5} mol dm^{-3}, pH 2.0) during 24 h. The inserted optical absorption spectra were measured simultaneously at the indicated applied potentials.

Potential dependent optical absorption spectroscopy of modified transparent nanostructured TiO_2 membranes

Fig. 3 shows the potential dependent optical absorption at 606 nm of a transparent nanostructured TiO_2 membrane prior to and following modification by chemisorption of $\mathbf{R^PV^{C4}}$. Also shown as inserts are the optical absorption spectra of this membrane measured at the indicated applied potentials.

For the unmodified transparent nanostructured TiO_2 membrane, the absorbance measured at 606 nm increases at applied potentials more negative than *ca.* −0.70 V. This absorbance increase is assigned, based on the spectrum measured at −0.90 V, principally to electrons trapped in surface Ti^{IV} states.[32] Significantly, on reversing the potential sweep there is only a small decrease in the absorbance measured at 606 nm on the time-scale of the reported experiment.

In the case of TiO_2–$\mathbf{R^PV^{C4}}$ the absorbance measured at 606 nm increases at applied potentials more negative than *ca.* −0.65 V. This increase in absorbance is assigned, based on the spectrum measured at −0.90 V, principally to the radical cation of **V** component.[33] The absorbance measured at 606 nm decreases at applied potentials more negative than *ca.* −0.77 owing to conversion of the radical cation of the **V** component to the corresponding neutral diradical.[33] On reversing the potential sweep, there is an initial increase in absorbance at 606 nm as the neutral diradical of the **V** component is reoxidized to the singly reduced form. At still more positive potentials, however, there is only a small decrease in the absorbance measured at 606 nm on the time-scale of the reported experiment. Qualitatively and quantitatively similar findings were obtained for TiO_2–$\mathbf{R^PV^{C1}}$.

Using the known absorption coefficient of the $\mathbf{R^P}$ component in TiO_2–$\mathbf{R^PV^{C1}}$ and TiO_2–$\mathbf{R^PV^{C4}}$,[17] it is possible to calculate the concentration of **V** components adsorbed at the surface of a nanostructured TiO_2 membrane.[34] Having done this, it is also possible to calculate the fraction of **V** components that are reduced at a given applied potential in TiO_2–$\mathbf{R^PV^{C1}}$ or TiO_2–$\mathbf{R^PV^{C4}}$. These findings are summarized in Table 1.

Irradiation dependent optical absorption spectroscopy of modified transparent nanostructured TiO_2 membranes

Fig. 4 shows the optical absorption spectra of a nanostructured TiO_2 membrane modified by chemisorbed $\mathbf{R^PV^{C4}}$ prior to and following irradiation at the indicated applied potentials with the blue–green output of an argon-ion laser.

It may be concluded from the spectra measured prior to irradiation at 0.00 and −0.60 V that there are no electrons trapped in surface Ti^{IV} states or reduced **V** components in TiO_2–$\mathbf{R^PV^{C4}}$. Following irradiation, however, there is a small but reproducibly measurable increase in the concentration of both. It may also be concluded from the spectrum measured at −0.65 V, again prior to irradiation, that there are electrons trapped in surface Ti^{IV} states and that a fraction of the **V** components in TiO_2–$\mathbf{R^PV^{C4}}$ are reduced. Following irradiation, there is a large increase in the fraction of the **V** components in TiO_2–$\mathbf{R^PV^{C4}}$ that are reduced (Table 1). Finally, it is clear from the spectrum measured at −0.70 V that all the **V** components in TiO_2–$\mathbf{R^PV^{C4}}$ that have the required geometry with respect to the constituent nanocrystals of the nanostructured membrane have been reduced. As a result, irradiation does not result in a further increase in the concentration of reduced **V** components (Table 1).

As may be seen from Fig. 5 and Table 2, it is not only the fraction of **V** components in TiO_2–$\mathbf{R^PV^{C4}}$ that are reduced following irradiation that depends on the applied potential, but also the lifetime of the radical cations formed. Specifically, the rate of decay of the reduced **V** at an applied potential of 0.00 V

Table 1 Percentage of **V** component in TiO_2–$\mathbf{R^PV^{C4}}$ and TiO_2–$\mathbf{R^PV^{C1}}$ reduced at the indicated applied potential prior to and following irradiation for 3 s using the blue–green output of an Ar-ion laser (1000 W cm^{-2})

	Applied potential/V				
	0.00	−0.60	−0.65	−0.70	−0.80
TiO_2–$\mathbf{R^PV^{C4}}$ (58 μm)					
Before irradiation	0	0	4	37	37
After irradiation (%)	4	5	31	37	37
TiO_2–$\mathbf{R^PV^{C1}}$ (58 μm)					
Before irradiation	0	0	0	40	40
After irradiation	13	13	19	40	40

depends on the applied potentials at which the reduced **V** component was generated.

As may be seen from the normalized data in Fig. 5, the radical cations generated at −0.70 and −0.65 V persist on the time scale of hours, while those generated at −0.60 and −0.00 V persist on the time scale of minutes.

Similar findings to those reported above were obtained for TiO_2–$\mathbf{R^PV^{C1}}$. These findings are also summarized in Tables 1 and 2.

Irradiation dependent optical absorption spectroscopy of molecular components in solution

The optical absorption spectra of $\mathbf{R^PV^{C1}}$ and $\mathbf{R^PV^{C4}}$ have been measured prior to and following irradiation of a solution (1.7×10^{-4} mol dm^{-3}) of these complexes in MeCN–EtOH (3 : 1, v/v) containing added $LiClO_4$ (0.2 mol dm^{-3}) and TEOA (0.05 mol dm^{-3}) with the blue–green output of an argon-ion laser (1000 mW cm^{-2}). Despite the fact that the absorbance at 460 nm of these solutions (2.5) matched those of TiO_2–$\mathbf{R^PV^{C1}}$ and TiO_2–$\mathbf{R^PV^{C4}}$ (Fig. 2), no measurable change in the optical absorption spectrum of either was observed. This finding, however, was not unexpected since the rate constants for back electron transfer from the reduced **V** component to the oxidized $\mathbf{R^P}$ component in $\mathbf{R^PV^{C1}}$ and $\mathbf{R^PV^{C4}}$ are 8.38×10^{10} s^{-1} and 3.24×10^9 s^{-1} respectively,[28,31] while the estimated diffusion limited effective first-order rate constant for electron transfer by the sacrificial donor TEOA to the oxidized $\mathbf{R^P}$ component is *ca.* 5×10^7 s^{-1}.[35] In short, electron transfer by the reduced **V** component to the oxidized $\mathbf{R^P}$ component in either $\mathbf{R^PV^{C1}}$ or $\mathbf{R^PV^{C4}}$ is more than two orders of magnitude faster than electron transfer by the sacrificial donor TEOA to the oxidized $\mathbf{R^P}$ component. As a result, the quantum efficiency for reduction of the **V** component in either $\mathbf{R^PV^{C1}}$ or $\mathbf{R^PV^{C4}}$ is $< 10^{-2}$ and no significant change in the absorption spectrum is measured.

Discussion

In order to account for the above observations the findings of studies in which the potential dependent optical absorption spectroscopy of transparent nanostructured TiO_2 films supported on conducting glass have been measured in a range of protic and aprotic solvents are considered.[17,32,36] These studies have established that, under the conditions for which these finding are reported, the potential of the conduction band edge (V_{cb}) at the semiconductor–liquid electrolyte interface (SLI) is −1.20 V. Consistent with the measured onset for bandgap absorption at 380 nm in Fig. 2, the potential of the valence band edge (V_{vb}) at the SLI is +2.06 V. Furthermore, it is known that there are two populations of intraband states in nanostructured TiO_2 films.[21] The first of these lies about 0.5 eV below the conduction band edge at −0.70 V and is assigned to surface Ti^{IV} states. The second of these lies about 1.63 eV below the conduction band edge and is assigned to surface peroxy species. From the above, and from the known half-wave potentials of the $\mathbf{R^P}$ and **V** components,[37] the energy level diagram in Scheme 5 may be constructed.

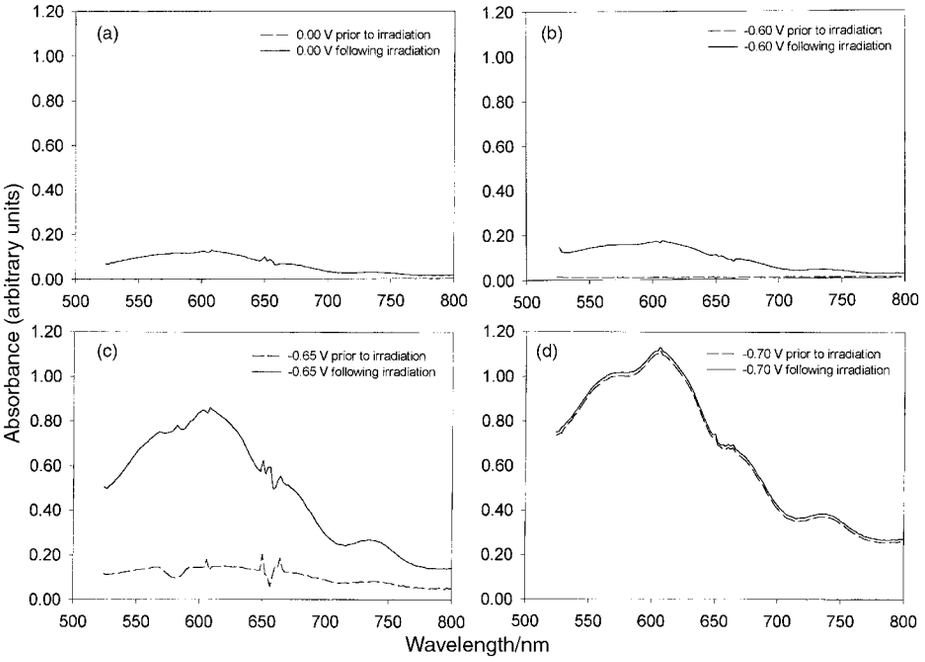

Fig. 4 Potential dependent optical absorption spectra of a 58 μm thick nanostructured TiO_2 membrane fired for 24 h and modified by adsorption of $\mathbf{R^PV^{C4}}$ from a saturated ethanolic solution (2×10^{-5} mol dm^{-3}, pH 2.0) during 24 h. The plotted spectra were recorded at the indicated applied potentials prior to and following irradiation for 3 s using the blue–green output of an Ar-ion laser (1000 mW cm^{-2}).

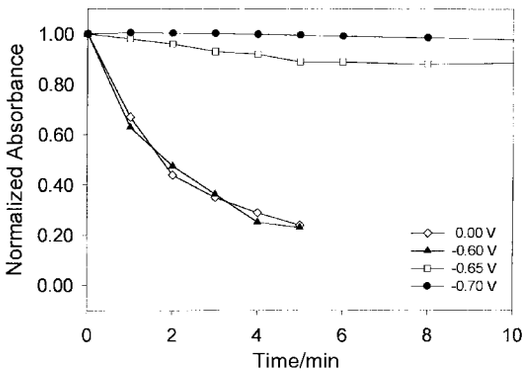

Fig. 5 Decay at 0.00 V of normalized absorbance at 606 nm assigned to reduced **V** component in TiO_2–$\mathbf{R^PV^{C4}}$ following irradiation at the indicated applied potential for 3 s using the blue–green output of an Ar-ion laser (1000 mW cm^{-2}).

It has been established that the increase in absorbance at applied potentials more negative than −0.65 V is due to formation of the radical cation of the **V** component in either TiO_2–$\mathbf{R^PV^{C1}}$ or TiO_2–$\mathbf{R^PV^{C4}}$ (Fig. 3). It has also been established that there is a population of surface Ti^{IV} states at −0.70 V and that the half-wave potential for the first reduction of the **V** component is −0.41 V (Scheme 5). On this basis it is concluded that reduction of the **V** component is mediated by surface Ti^{IV} states.[38]

As was noted, only 37 and 40% of the **V** components in TiO_2–$\mathbf{R^PV^{C4}}$ and TiO_2–$\mathbf{R^PV^{C1}}$ respectively are reduced (Table 1). This suggests that only a fraction of these **V** components have the required orientation with respect to the constituent nanocrystals of the membrane substrate to be reduced. The fact that a larger fraction of the **V** components in TiO_2–$\mathbf{R^PV^{C4}}$ are reduced, compared to TiO_2–$\mathbf{R^PV^{C1}}$, further supports this assertion.[16,17,20]

It has been established that the decrease in absorbance at 600 nm between −0.77 and −0.90 V is due to formation of neutral dication of the **V** component in TiO_2–$\mathbf{R^PV^{C1}}$ and TiO_2–$\mathbf{R^PV^{C4}}$ (Fig. 3). It has also been established that there is a population of surface Ti^{IV} states at −0.70 V and that the half-wave potential for the second reduction of the **V** component is −0.81 V (Scheme 5). On this basis it is concluded that second reduction of the **V** component is also mediated by surface Ti^{IV} states.[38]

On reversing the applied potential, the surface Ti^{IV} states are emptied and this results in the neutral diradical of the **V** component in TiO_2–$\mathbf{R^PV^{C1}}$ and TiO_2–$\mathbf{R^PV^{C4}}$ being reoxidized to the highly colored radical cation (Fig. 3). Clearly, the concentration of surface Ti^{IV} states at potentials more positive than −0.41 V, the half-wave potential for the first reduction of the **V** component, is negligible (Scheme 5). As a consequence, reoxidation of the radical cation to the dication is a slow process and the absorbance assigned to this species persists for some hours even at 0.00 V (Fig. 3).

Blue–green irradiation of TiO_2–$\mathbf{R^PV^{C1}}$ or TiO_2–$\mathbf{R^PV^{C4}}$ results in the formation of radical cations of the **V** component that are long-lived (Fig. 4 and 5). The following, however, is noted: first, that the fraction of the **V** components which are reduced and the extent to which they are long-lived is dependent on the potential applied to the transparent nanostructured TiO_2 membrane; and second, that irradiation of either $\mathbf{R^PV^{C1}}$ or $\mathbf{R^PV^{C4}}$ under similar conditions in solution does not result in the formation of radical cations of the **V** component that are long-lived. On this basis it is concluded that formation of radical cations of the **V** component that are long-lived is as a result of electron transfer mediated by the surface Ti^{IV} states of the transparent nanostructured TiO_2 membrane, and is not as a result of electron transfer from the electronically excited **R** component to the **V** component. Those radical cations which are formed by electron transfer from the electronically excited **R** complex to the **V** component are short lived as regeneration of the oxidized **R** component by TEOA does not compete with back electron transfer from the reduced **V** component.

Table 2 First order rate constant for reoxidation of the reduced **V** component in TiO_2–$\mathbf{R^PV^{C4}}$ and TiO_2–$\mathbf{R^PV^{C1}}$ at 0.00 V following irradiation for 3 s using the blue–green output of an Ar-ion laser (1000 mW cm^{-2}) at the indicated applied potential

	Applied potential/V				
	0.00	−0.60	−0.65	−0.70	−0.80
TiO_2–$\mathbf{R^PV^{C4}}$ (58 μm)					
$10^4\ k/s^{-1}$	4.7	49	1.3	0.5	—
TiO_2–$\mathbf{R^PV^{C1}}$ (58 μm)					
$10^4\ k/s^{-1}$	4.5	—	2.8	4.1	—

The following mechanism is proposed to account for long-lived light-induced charge separation: Absorption of a visible photon by the $\mathbf{R^P}$ component in either TiO_2–$\mathbf{R^PV^{C1}}$ or TiO_2–$\mathbf{R^PV^{C4}}$ results in electron transfer to a conduction band state of the TiO_2 nanocrystal component with 95% efficiency. The injected electrons are subsequently trapped at surface Ti^{IV} states and the rate of back electron transfer slowed.[27,30] As a consequence, the oxidized $\mathbf{R^P}$ component is principally regenerated by electron transfer from the sacrificial donor TEOA.[24,27] Continuous irradiation leads to an increase in the concentration of electrons trapped at surface Ti^{IV} states and a corresponding increase in the magnitude of the shift of the quasi-Fermi level of the TiO_2 nanocrystal component to negative potentials. Eventually, the quasi-Fermi level of the TiO_2 nanocrystal component is shifted to sufficiently negative potentials to reduce the **V** component in either TiO_2–$\mathbf{R^PV^{C1}}$ or TiO_2–$\mathbf{R^PV^{C4}}$. It should be noted that since the radical cation of the **V** component is formed only where TiO_2–$\mathbf{R^PV^{C1}}$ or TiO_2–$\mathbf{R^PV^{C4}}$ are irradiated, the shift of the quasi-Fermi level to more negative potentials is apparently localized. This mechanism is summarized in Scheme 6.

Consistent with the proposed mechanism is the observation that irradiation of either TiO_2–$\mathbf{R^PV^{C1}}$ or TiO_2–$\mathbf{R^PV^{C4}}$ at applied potentials positive of the potential of the surface Ti^{IV} states (0.00 V), results in a small shift in the quasi-Fermi level to more negative potentials and in a small increase in the fraction of **V** components that are reduced (Fig. 4, Table 1). At more negative applied potentials (−0.65 V), these surface Ti^{IV} states are filled and irradiation results in a large shift in the quasi-Fermi level to more negative potentials and in a large fraction

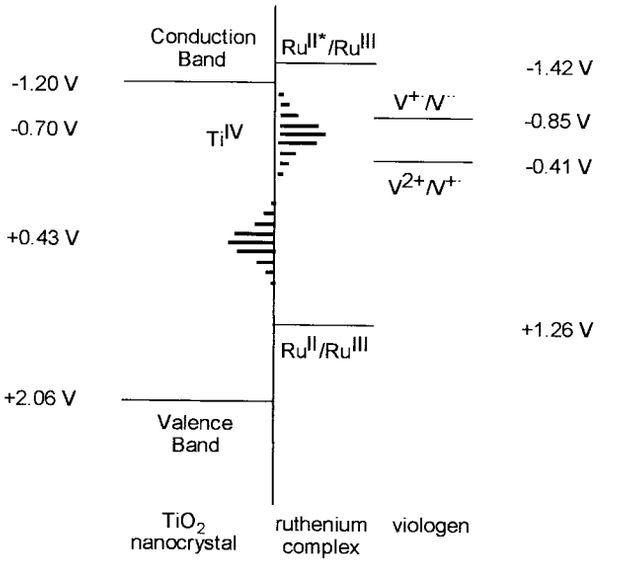

Scheme 5

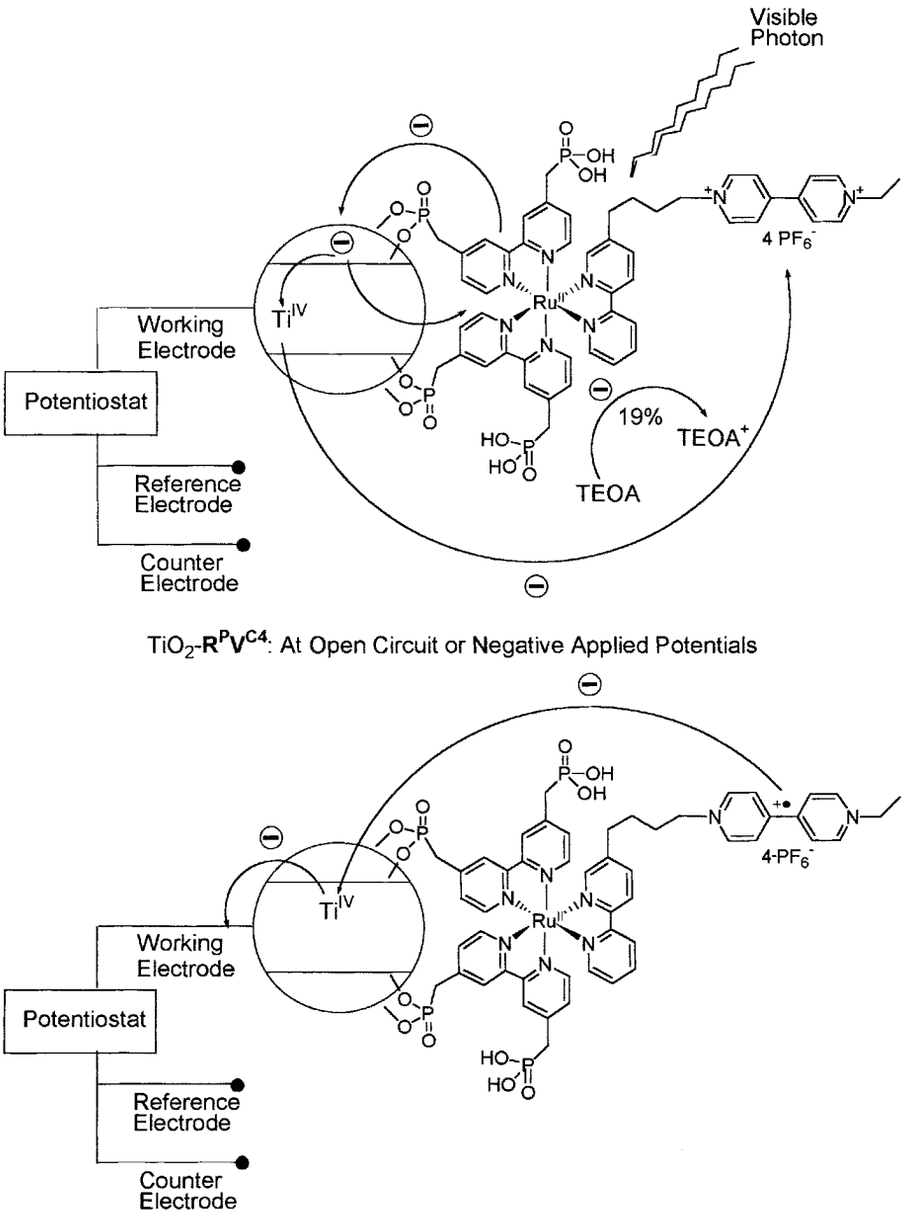

Scheme 6

of the **V** components in both TiO_2–$\mathbf{R^PV^{C1}}$ and TiO_2–$\mathbf{R^PV^{C4}}$ being reduced. At still more negative applied potentials (−0.70 V) all **V** components with the requisite geometry in either TiO_2–$\mathbf{R^PV^{C1}}$ or TiO_2–$\mathbf{R^PV^{C4}}$ have been reduced and optically pumping the quasi-Fermi potential to more negative potentials does not result in an increase in the fraction of **V** components that are reduced. It should be noted that in the potential sweep data reported in Fig. 3, all the **V** components are reduced at applied potentials more negative than −0.77 V, this difference is accounted for by the fact that trap mediated electron transfer is slow.

Also consistent with the proposed mechanism is the observation that for both TiO_2–$\mathbf{R^PV^{C1}}$ and TiO_2–$\mathbf{R^PV^{C4}}$ the rate of reoxidation of the **V** component is slowest for radical cations generated at negative applied potentials as a consequence of the surface Ti^{IV} states being filled (Fig. 5, Table 2).[5,29] As has been noted the rate of reoxidation of the **V** component in TiO_2–$\mathbf{R^PV^{C1}}$ is slower than the rate of reoxidation of the **V** component in $\mathbf{TiO_2}$–$\mathbf{R^PV^{C4}}$ at a given applied potential. It is tentatively suggested that this is accounted for by the reduced mobility of the **V** component in TiO_2–$\mathbf{R^PV^{C1}}$ compared with that of the same component in TiO_2–$\mathbf{R^PV^{C4}}$.

Finally, the differences between the findings reported here for TiO_2–$\mathbf{R^PV^{C4}}$ and TiO_2–$\mathbf{R^PV^{C1}}$ and those reported for the closely related heterosupramolecular assemblies described in ref. 17 are accounted for as follows: the heterosupramolecular assemblies in ref. 17 are based on nanostructured TiO_2 films supported on conducting glass and modified by chemisorbed $\mathbf{R^PV^{C4}}$ and TiO_2–$\mathbf{R^PV^{C1}}$. Furthermore, these heterosupramolecular assemblies are immersed in aqueous electrolytes at pH 2.0. As a consequence of the above, the density of trap states is significantly lower (characterizing of supported films due to better thermal contact during firing[20]) and V_{cb} is at significantly more positive potential and is important in mediating electron transfer to and from the **V** component.

Conclusions

Heterosupermolecules have been assembled by covalently linking a TiO_2 nanocrystal, a ruthenium complex and a

viologen. The covalent organization of these heterosupermolecules yields the heterosupramolecular assemblies TiO_2–$\mathbf{R^PV^{C4}}$ and TiO_2–$\mathbf{R^PV^{C4}}$. Their associated heterosupramolecular function, long-lived light-induced charge separation leading to formation of the reduced form of **V** component, may be modulated potentiostatically.

In practice, exposure of these heterosupramolecular assemblies to visible light causes them to turn blue. Furthermore, if a negative potential is applied to the nanostructured TiO_2 membrane this blue color persists for hours. Because it is only those areas that have been irradiated that are blue, and because the lifetime of the blue coloration depends on the potential applied to the nanostructured TiO_2 membrane, applications are foreseen for these photoelectrochromic materials.[39]

Acknowledgements

These studies were supported by a grant from the Commission of the European Union under the Training and Mobility of Researchers (Network) Program (Contract FMRX CT96-0076). J.S. wishes to thank the Fundacao para a Ciencia e Tecnologia for funding in part his stay at University College Dublin.

References

1 J.-M. Lehn, *Supramolecular Chemistry*, VCH, New York, 1995.
2 V. Balzani and F. Scandola, *Supramolecular Chemistry*, Ellis Horwood, New York, 1991.
3 X. Marguerettaz, L. Cusack and D. Fitzmaurice, *Nanoparticle Characterizations and Utilizations*, ed. J. Fendler, VCH-Wiley, New York, 1998, ch. 16; S. N. Rao and D. Fitzmaurice, *Helv. Chim. Acta*, 1998, **81**, 902; X. Marguerettaz, A. Merrins and D. Fitzmaurice, *J. Mater. Chem.*, 1998, **10**, 2157.
4 Y. Athanassov, F. Rotzinger, P. Pechy and M. Grätzel, *J. Phys. Chem. B*, 1997, **101**, 2558; P. Bonhote, J. Moser, N. Vlachopoulos, L. Walder, S. Zakeeruddin, R. Humphry-Baker, P. Pechy and M. Grätzel, *Chem. Commun.*, 1996, 1163; P. Bonhote, E. Gogniat, S. Tingry, C. Barbe, N. Vlachopoulos, F. Lenzmann, P. Compte and M. Grätzel, *J. Phys. Chem. B*, 1998, **102**, 1498.
5 X. Marguerettaz, R. O'Neill and D. Fitzmaurice, *J. Am. Chem. Soc.*, 1994, **116**, 2628; L. Cusack, S. N. Rao and D. Fitzmaurice, *Chem. Eur. J.*, 1997, **3**, 202; L. Cusack, R. Rizza, A. Gorelov and D. Fitzmaurice, *Angew. Chem., Int. Ed. Engl.*, 1997, **36**, 848.
6 J.-M. Lehn, *Angew. Chem., Int. Ed. Engl.*, 1988, **27**, 89.
7 G. Ashwell, *Molecular Electronics*, Wiley, New York, 1992.
8 J. Hopfield, J. Nelson-Onuchic and D. Beretan, *Science*, 1988, **241**, 817.
9 F. Vöglte, W. Müller, U. Müller, M. Bauer and K. Rissanen, *Angew. Chem., Int. Ed. Engl.*, 1993, **32**, 1295.
10 R. Bissel, E. Cordova, A. Kaifer and J. F. Stoddart, *Nature*, 1994, **369**, 133.
11 A. P. de Silva, H. Nimal Gunaratne and C. Mc Coy, *Chem. Commun.*, 1996, 2399.
12 P. Avouris, *Acc. Chem. Res.*, 1995, **28**, 95.
13 P. Alivisatos, *Science*, 1996, **271**, 933.
14 X. Marguerettaz and D. Fitzmaurice, *J. Am. Chem. Soc.*, 1994, **116**, 5017.
15 X. Marguerettaz, G. Redmond, S. N. Rao and D. Fitzmaurice, *Chem. Eur. J.*, 1996, **2**, 420.
16 G. Will, G. Boschloo, R. Hoyle, S. N. Rao and D. Fitzmaurice, *J. Phys. Chem. B*, 1998, **102**, 10272.
17 G. Will, R. Boschloo, S. N. Rao and D. Fitzmaurice, *J. Phys. Chem. B*, 1999, **103**, 8067.
18 G. Will, R. Boschloo, S. N. Rao and D. Fitzmaurice, *J. Mater. Chem.*, 1999, **9**, 2297.
19 R. Cinnsealeach, G. Boschloo, S. N. Rao and D. Fitzmaurice, *Sol. Energy Mater. Sol. Cells*, 1999, **57**, 107.
20 R. Hoyle, J. Sotomayor, G. Will and D. Fitzmaurice, *J. Phys. Chem. B*, 1997, **101**, 10791; J. Sotomayor, R. Hoyle, G. Will and D. Fitzmaurice, *J. Mater. Chem.*, 1998, **8**, 105; R. Hoyle, G. Will and D. Fitzmaurice, *J. Mater. Chem.*, 1998, **8**, 2003.
21 H. Finklea, *Semiconductor Electrodes*, Elsevier, New York, 1988.
22 The concentration of $\mathbf{R^PV^{C4}}$ adsorbed at the surface of a 58 μm thick nanostructured TiO_2 membrane was calculated to be 1×10^{17} molecules cm^{-2} based on an absorption coefficient of 14 200 mol^{-1} dm^3 cm^{-1} [17] and an absorbance of 2.5, both measured at 450 nm. Assuming the concentration of surface Ti^{IV} states is 2×10^{13} cm^{-2}, this suggests a surface roughness of *ca.* 5300.
23 K. Kalyanasundaram, *Coord. Chem. Rev.*, 1982, **46**, 159.
24 A. Juris, V. Balzani, F. Barigelletti, S. Campagna, P. Belser and A. Von Zelewsky, *Coord. Chem. Rev.*, 1988, **84**, 85.
25 N. Damrauer, G. Cerullo, A. Yeh, T. Boussie, C. Shank and J. McCusker, *Science*, 1997, **275**, 54.
26 L. DeArmond, K. Hanck and D. Wertz, *Coord. Chem. Rev.*, 1985, **64**, 65.
27 B. O'Regan and M. Grätzel, *Nature*, 1991, **353**, 737; M. K. Nazeerudin, A. Kay, I. Rodicio, R. Humphry-Baker, E. Muller, P. Liska, N. Vlachopoulos and M. Grätzel, *J. Am. Chem. Soc.*, 1993, **115**, 6382.
28 E. Yonemoto, R. Riley, Y. Kim, S. Atherton, R. Schmehl and T. Mallouk, *J. Am. Chem. Soc.*, 1992, **114**, 8081; E. Yonemoto, G. Saupe, R. Schmehl, S. Hubig, R. Riley, B. Iverson and T. Mallouk, *J. Am. Chem. Soc.*, 1994, **116**, 4786.
29 X. Xu, K. Shreder, B. Iverson and A. Bard, *J. Am. Chem. Soc.*, 1996, **118**, 3656.
30 Y. Tachibana, J. Moser, M. Grätzel, D. Klug and J. Durrant, *J. Phys. Chem.*, 1996, **100**, 20056; T. Hannappel, B. Burnfeindt, W. Storck and F. Willig, *J. Phys. Chem. B*, 1997, **101**, 6977; R. Ellingson, J. Asbury, S. Ferrere, H. Ghosh, J. Sprague, T. Lian and A. Nozik, *J. Phys. Chem. B*, 1998, **102**, 6455.
31 P. Ashton, R. Ballardini, V. Balzani, E. Constable, A. Credi, O. Kocian, S. Langford, J. Preece, L. Prodi, E. Schofield, N. Spencer, J. F. Stoddart and S. Wenger, *Chem. Eur. J.*, 1998, **4**, 2413.
32 D. Fitzmaurice, *Sol. Energy. Mater. Sol. Cells*, 1994, **32**, 289; G. Rothenberger, D. Fitzmaurice and M. Grätzel, *J. Phys. Chem.*, 1992, **96**, 5983.
33 B. Kok, H. Rurainski and O. Owens, *Biochim. Biophys. Acta*, 1965, **109**, 347; P. Trudinger, *Anal. Biochem.*, 1970, **36**, 222; T. Wantanabe and K. Honda, *J. Phys. Chem.*, 1982, **86**, 2617.
34 The values in Table 1 were calculated assuming the ratio between the number of ruthenium complex components and **V** components was 1 : 1. It was also assumed that the absorption coefficients for these components are 14 500 mol^{-1} dm^3 cm^{-1} at 457 nm[17] and 13 700 mol^{-1} dm^3 cm^{-1} at 606 nm,[32] respectively.
35 The concentration of $\mathbf{R^PV^{C4}}$ and $\mathbf{R^PV^{C1}}$ in MeCN/EtOH (3 : 1, v/v) was 1.7×10^{-4} mol dm^{-3}, while the concentration of TEOA was 0.05 mol dm^{-3}. Assuming all **R** are oxidized and a diffusion limited rate constant for MeCN–EtOH of 10^9 mol^{-1} dm^3 s^{-1}, an upper limit for the effective first-order rate constant of 5×10^7 s^{-1} is estimated.
36 G. Redmond and D. Fitzmaurice, *J. Phys. Chem.*, 1993, **97**, 1426; B. Enright, G. Redmond and D. Fitzmaurice, *J. Phys. Chem.*, 1994, **98**, 6195.
37 G. Will, G. Boschloo, S. N. Rao, D. Fitzmaurice, T. McCormack, A. Lees, R. Forster, J. Vos, C. Kleverlaan and F. Scandola, in preparation.
38 H. Frei, D. Fitzmaurice and M. Grätzel, *Langmuir*, 1990, **6**, 198.
39 G. Will, J. Sotomayor, S. N. Rao and D. Fitzmaurice, in preparation.

Paper a908064c